FORMATION AND DECAY OF HOT NUCLEI IN HEAVY ION COLLISIONS*

R. Płaneta[a], W. Gawlikowicz[a], K. Grotowski[a,d]
J. Brzychczyk[a], T. Ciszek[a], A.J. Cole[b], P. Désesquelles[b]
S. Micek[a], P. Pawłowski[a], Z. Sosin[a], A. Wieloch[a]
D. Benchekroun[c], E. Bisquer[c], A. Chabane[b], M. Charvet[b]
B. Cheynis[c], A. Demeyer[c], E. Gerlic[c], A. Giorni[b], D. Guinet[c]
D. Heuer[b], P. Lautesse[c], L. Lebreton[c], A. Lléres[b], M. Stern[c]
L. Vagneron[c], and J.B. Viano[b]

[a]M. Smoluchowski Institute of Physics, Jagellonian University
Reymonta 4, 30-059 Cracow, Poland
[b]Institut des Sciences Nucléaires de Grenoble, IN2P3-CNRS/ Université
Joseph Fourier 53, Avenue des Martyrs, 38026 Grenoble Cedex, France
[c]Institut de Physique Nucléaire de Lyon, IN2P3-CNRS/Université Claude
Bernard 43, Boulevard du 11 Novembre 1918, 69622 Villeurbanne Cedex, France
[d]H. Niewodniczański Institute of Nuclear Physics
Radzikowskiego 152, 31-342 Cracow, Poland

(Received April 4, 2000)

The properties of the multifragmentation of "hot sources" produced in the ^{40}Ca+^{40}Ca reaction have been studied at a beam energy 35 MeV/nucleon. Two signatures of prompt multifragmentation, which make use of special features of particle emission from the "freeze out volume", together with an analysis of the reduced relative velocity between pairs of intermediate mass fragments, indicate the presence of a transition from sequential decay to prompt multifragmentation at an excitation energy of about 3 MeV/nucleon.

PACS numbers: 25.70.Gh, 25.70.Lm, 25.70.Pq

1. Introduction

Phase transitions in finite systems are presently a subject of great interest. Prompt multifragmentation of highly excited nuclei is of particular interest, since it may yield information concerning the liquid-gas phase transition in nuclear matter [1]. The latter may be induced by a nuclear collision

* Presented at the Kazimierz Grotowski 70$^{\rm th}$ Birthday Symposium "Phases of Nuclear Matter", Kraków, Poland, January 27–28, 2000.

transferring a system into a spinodal region of instability [2]. Multifragmentation may also appear as a natural extrapolation of the evaporation mechanism characteristic of nuclear decay at low excitation energies. The essential question concerns the typical time interval between successive emissions. In the limit of very short times nuclear multifragmentation can be considered as prompt multifragmentation (PM), whereas the opposite limit is usually referred to as a sequential or a binary sequential decay (BSD).

At low excitation energies ($\cong$ 2MeV/nucleon), atomic nuclei decay by the emission of neutrons and light charged particles. In this scenario particle emission is such a rare event that a chain of subsequent emissions may be assumed to take place from a corresponding sequence of equilibrated parent nuclei. With increasing energy the emission of heavier particles, intermediate mass fragments (IMF, $Z > 2$) competes with light particle emission. The assumption of step by step equilibration of parent nuclei may break down with further increase of the excitation energy and reduction of the decay time scales, since the parent nucleus may not have time to equilibrate between successive emissions [3]. Emitted particles may not have time to leave the vicinity of the parent and consequently the presence of previously emitted fragments may influence the decay process.

At excitation energy high enough to transfer a nuclear system into the spinodal region, the system should break into fragments due to the instability of nuclear matter. In this case one can postulate the existence of a set of fragments, enclosed in some finite spatial region (the "freeze-out volume"), which interact only via the inter-fragment repulsive Coulomb force [4]. Although such a process is considered to be prompt, it should not be treated as simply a short-time-limit of the sequential decay.

The experimental search for differences between the BSD and PM processes is usually based on dynamic correlations between the IMFs emitted from a nuclear system [5]. IMFs from PM are localized closer in space and in time as compared to IMFs from BSD. Consequently, at small values of the relative velocity, the number of coincidences is smaller for PM than for BSD. In the above method the main difference between BSD and PM is due to the decay time.

In this work we make use of two novel signatures of prompt multifragmentation, which, instead of the decay time, exploit special features of particle emission from the "freeze out volume". These are: *(i)* the shape of the distribution of squared momentum of the heaviest emitted fragment, p_1^2, [6,7], *(ii)* the focusing of fragments of the decaying system by the Coulomb field [8].

A recursion relation has been derived by Cole [6], which relates the mean square momenta of the sequentially emitted light particles and of the final residue. It appears that the mean square momentum of the residue is always smaller than the mean of the sum of the squares of the momenta of sequentially emitted particles.

The situation is quite different for prompt multifragmentation. In this case the heaviest fragment receives a collective Coulomb "kick" from other particles contained inside the "freeze out volume". Simulation shows that the mean value of p_1^2 for the sequential decay scenario is smaller than the mean value of p_1^2 in the case of prompt multifragmentation [7].

The second signature, the Coulomb focusing effect, was proposed by Gawlikowicz [8]. For prompt multifragmentation from a single hot source, momentum conservation tends to generate back-to-back motion of the two heaviest fragments, producing axial Coulomb focusing of the light charged particles. In the case of sequential decay this focusing effect is much weaker.

In Section 2 the reconstruction procedure of hot sources is described. These sources are: projectile-like fragments (PLFs) produced in deep inelastic collisions (DICs), and composite systems (CSs) resulting from incomplete fusion. A model describing the creation and decay of such "hot sources" is briefly presented in Section 3. The decay characteristics of "hot" PLFs and CSs are studied in Sections 4 and 5, respectively. The last section contains a summary and conclusions.

2. The ^{40}Ca + ^{40}Ca experiment and data

The experiment was performed at the Grenoble SARA facility using the AMPHORA upgraded multi-detector system [9,10]. For the symmetric ^{40}Ca + ^{40}Ca system most fragments are detected in the forward part of the detector, where the granularity of AMPHORA provides a good angular resolution for particle–particle correlation measurements. The experimental details are described in [11,12].

2.1. The PLF hot source

At 35 MeV/nucleon the dynamics of peripheral ^{40}Ca + ^{40}Ca collisions exhibits a predominantly binary mechanism characterized by strong energy dissipation [11–13]. Thus, in the exit channel, we should observe two excited and decaying "sources": a target-like and a projectile-like fragment (TLF and PLF). Because of kinematics and detection energy thresholds only a very small fraction of the TLF source is visible. Therefore in this paper we focus our attention on the reconstruction of primary PLFs. The PLF fragments charge, mass and excitation energy have been determined using the reconstruction procedure [13,14].

The angular distributions of fragments measured in the center of mass of the decaying PLF indicate forward-backward symmetry for the IMF emission, as expected for a thermalized source [13].

The reconstructed charge and excitation energy distributions of the primary PLF are presented in Fig. 1. As one can see, deep inelastic collisions produce a broad range of nuclei with an average charge of about 20, and excitation energies extending from zero up to over 10 MeV/nucleon. Such a span of excitation energy should make it possible to trace a transition from BSD to PM.

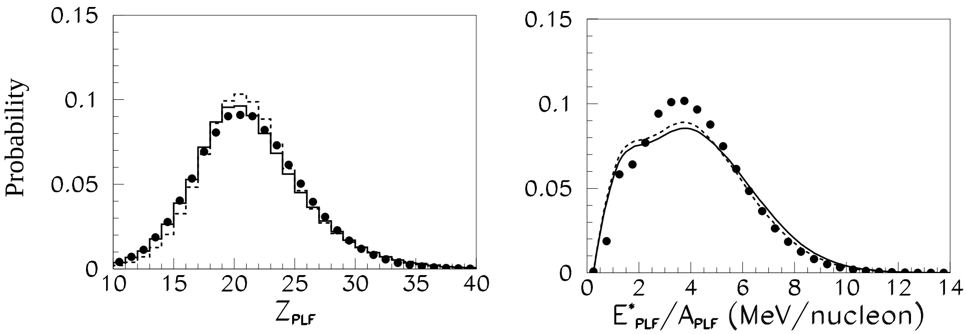

Fig. 1. The PLF reconstructed charge and excitation energy distributions (black dots), together with model predictions (PM — solid line; BSD — broken line).

2.2. The CS hot source

For more central collisions a composite system is formed as a result of incomplete fusion, with a very low cross section (several milibarns). To select events belonging to more central collisions we use a cut in the coplanarity (C) sphericity (S) plane [15]. Parameters C and S are related to the shape of the event in the linear momentum space. The cut is defined by:

$$C < 0.7(S - 0.3)\,. \tag{1}$$

In model simulations (see Sec. 3) we can tag events produced according to incomplete fusion or the DIC scenario and estimate their relative contributions. With the restriction (1) and additional conditions — total detected charge $Z_{\mathrm{total}} > 34$ and the LAB angle of the heaviest fragment $\Theta_1 < 20$ degrees — about 60 percent of events come from the incomplete fusion.

The total charge and excitation energy distributions of the primary "hot CS source" reconstructed under the above conditions are presented in Fig. 2. The charge distribution is concentrated in the region just below $Z = 40$. The CS excitation energy is quite high (about 8.5 MeV/nucleon), and the width of its distribution (the FWHM value) is about 3 MeV/nucleon.

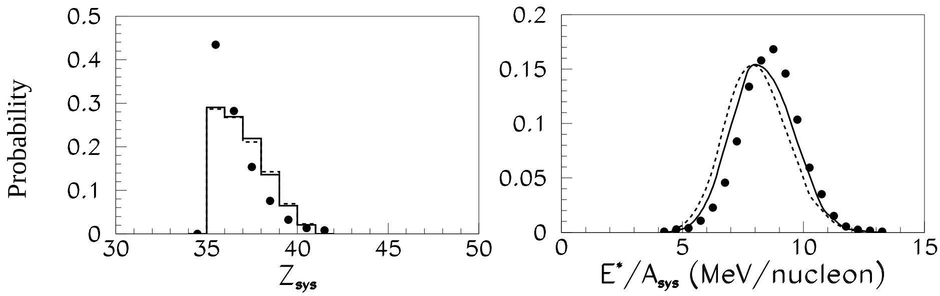

Fig. 2. The CS reconstructed charge and excitation energy distributions (black dots) together with model predictions (PM — solid line; BSD — broken line).

3. Simulation

In order to study different decay scenarios of "hot sources" one must use special gating techniques and particle correlation methods. To check them a model is needed which reproduces some necessary details of the reaction picture. We use a computer code elaborated by Sosin [16] which belongs to a family of models [17] based on the Randrup assumption [18] that at higher collision energies, energy dissipation proceeds mainly through stochastic transfer of nucleons between colliding ions.

Sosin computer code includes competition between mean field effects and the effects of nucleon–nucleon interactions in the overlap zone of colliding nuclei. The activated nucleons are transfered to PLF or TLF. They may also escape from the system or form a cluster. In the limit of smaller angular momenta (more central collisions) such a clustering process may result in the formation of a composite system.

An excited PLF, TLF or CS emits particles. In the model the deexcitation process is simulated by the GEMINI statistical code [19] which treats the cooling process as a sequence of binary decays.

As an option, the code permits decay of an excited PLF (TLF) or CS by prompt multifragmentation. In this work we follow a suggestion made by López and Randrup [4] and applied in our previous work [8]. For a given system with an initial angular momentum L and excitation energy E^* (obtained from the Sosin code) we use a partition provided by the GEMINI code as an initial distribution of fragments inside the "freeze-out" volume. The initial fragments are randomly positioned by a Monte Carlo subroutine [8,20] inside a spherical region of space such that no two fragments overlap. Energy, linear momentum, and angular momentum are conserved for each event.

The fragments of the initial configuration are accelerated in the mutual Coulomb field along proper trajectories, which are integrated numerically [21]. The predictions of the code are filtered by a software replica of the AMPHORA detector system [22]. For comparison with experimental data the same reconstruction procedure for a PLF or CS has been applied to the model predictions as for the data. Some of the results obtained using the above procedure are presented in Figs 1 and 2.

4. Decay characteristics of hot PLFs

To study the PLF decay characteristics one can use a conventional method based on correlations between the IMFs emitted from the excited PLF. Here we use a $1 + R(v_{\rm red})$ correlation function for pairs of IMFs moving apart with a reduced relative velocity, $v_{\rm red}$ [5].

The reduced velocity correlation functions measured for pairs of IMFs with $3 \leq Z \leq 8$ are shown in Fig. 3(a) for different bins of the excitation energy of the primary PLF. The "Coulomb hole" seen at small values of $v_{\rm red}$ clearly broadens for higher PLF excitation energies. The sequential

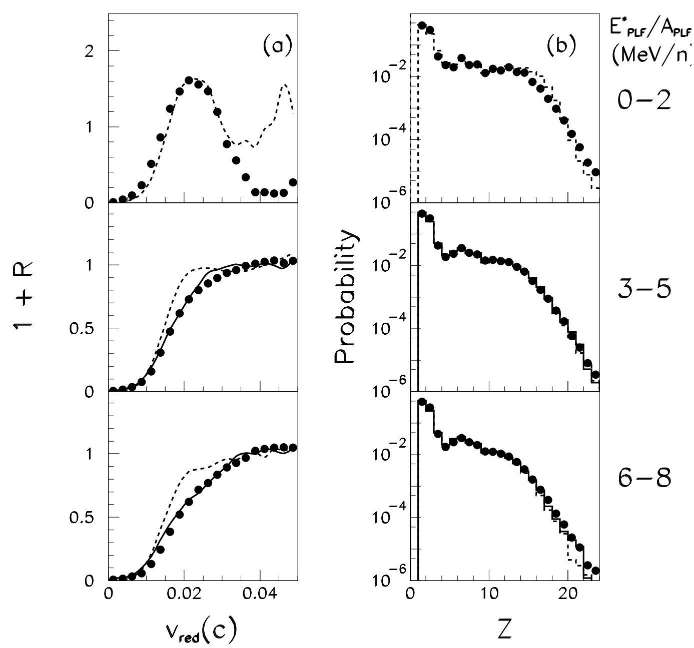

Fig. 3. Reduced velocity correlation functions for: (a) IMF's with $3 \leq Z \leq 8$, and (b) particle charge spectra, measured for different PLF excitation energy bins. Black dots indicate experimental data. Model predictions: solid line — PM; broken line — BSD.

binary scenario explains the experimental data at low excitations only, below 3 MeV/nucleon. At higher excitations one must use a correlation function calculated according to the PM scenario. The size of the "Coulomb hole" is similar to that measured for other systems at similar energies [23–25].

As seen from Fig. 3(b), the agreement of the measured Z distributions with model predictions is good, for both BSD and PM reaction scenarios and for all excitation energy bins.

As an alternative, instead of the $1 + R$ correlation method we can examine the distribution of the squared momentum of the heaviest fragment, p_1^2. For this signature fragment momenta should be measured in the PLF center of the mass system whose location is determined, event by event, in the PLF reconstruction procedure [13]. To avoid the influence of the TLF we take only those heaviest fragments which are emitted at an angle smaller than 90 degrees in the coordinate system oriented by the running PLF.

The measured distributions of the squared momentum p_1^2 of the heaviest fragment are displayed in Fig. 4. They become distinctly broader for PLF excitation energies higher than 3 MeV/nucleon, in agreement with the PM model prediction.

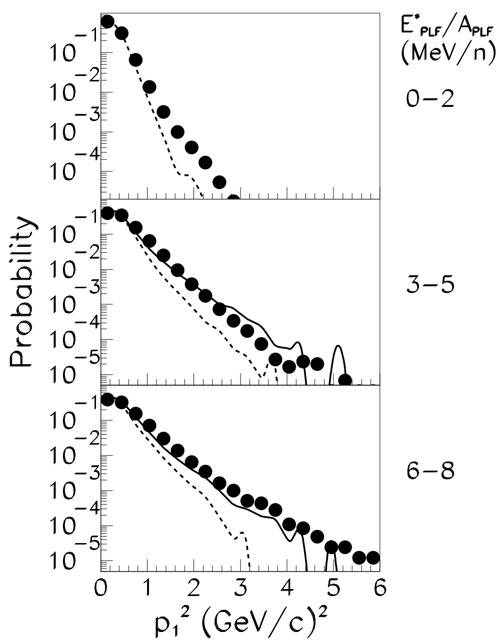

Fig. 4. Distributions of p_1^2 for different PLF excitation energy bins. Black dots indicate experimental data. Model predictions: solid line — PM; broken line — BSD.

5. Decay characteristics of hot CSs

Fig. 5(a) displays the $1+R$ correlation function for events selected by the conditions described in Sec. 2.2. It shows a broad "Coulomb hole" in agreement with the PM model prediction, but too broad for the BSD decay scenario. In this case also the size of the "Coulomb hole" is comparable with other results [23–25].

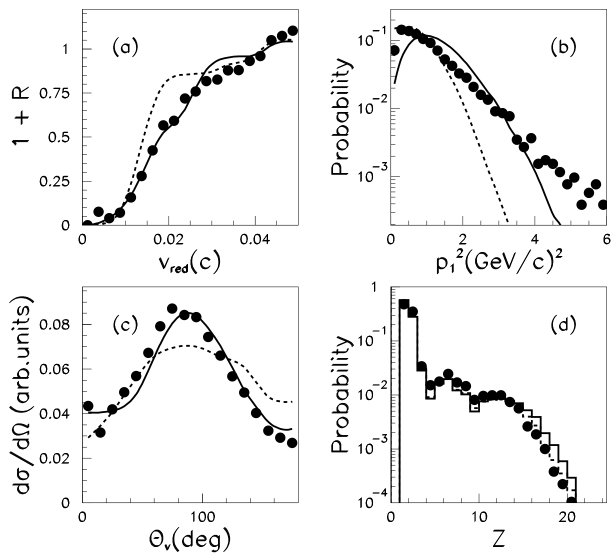

Fig. 5. Composite system: (a) $1+R$ correlation function; (b) p_1^2 distribution; (c) Coulomb focusing; (d) secondary charge distribution. Black dots indicate experimental data. Model predictions: solid line — PM; broken line — BSD.

The p_1^2 distribution (Fig. 5(b)) is well predicted by the PM reaction scenario, but is in disagreement with the BSD curve.

The Coulomb focusing effect is observed in the IMF velocity distribution, $d\sigma(\Theta_v)/d\Omega$, displayed in a reference frame defined by the relative velocity, $\vec{v}_1 - \vec{v}_2$, of the two heaviest fragments. Here Θ_v is an angle between the IMF velocity and the $\vec{v}_1 - \vec{v}_2$ vector. As expected the two heaviest fragments generate a strong Coulomb field, focusing the velocities of IMFs around $\Theta_v = 90$ degrees (see Fig. 5(c)). The experimental points agree with the PM prediction. For the sequential binary decay the $d\sigma(\Theta_v)/d\Omega$ distribution is distinctly flatter but not isotropic because of momentum conservation and very short time intervals between consecutive emissions, which create a dependence of subsequent decays.

The agreement of the measured Z distribution with the model prediction is good, for both BSD and PM reaction scenarios (see Fig. 5(d)). In spite of the nearly two times larger CS mass and charge, the Z distribution here is not longer than the PLF one, because of much higher average CS excitation.

6. Summary and conclusions

The multifragmentation of excited nuclei from the ^{40}Ca + ^{40}Ca reaction at $E_{\mathrm{LAB}} = 35$ MeV/nucleon has been studied using the AMPHORA multidetector system. Using special gating and reconstruction procedures we could observe projectile-like fragments with different degrees of excitation, and also highly excited systems from incomplete fusion. These "hot sources" possess features of thermalized systems. To investigate their decay characteristics we have used the conventional reduced velocity correlation method and also two signatures based on the distribution of the squared momentum of the heaviest fragment, and on the Coulomb focusing effect, respectively.

For the PLF, both methods, the reduced velocity correlation, and the p_1^2 distribution, support the binary sequential decay scenario below an excitation energy of 3 MeV/nucleon, and prompt multifragmentation for higher excitations. For a CS which has about twice the PLF electric charge the Coulomb focusing effect could also be observed. In that case all three signatures indicate prompt multifragmentation of the hot system.

The consistency of all these observations shows that both the p_1^2 distribution and the Coulomb focusing effect can be used as signatures of prompt multifragmentation.

At high excitations the PM signal (the difference between the BSD and PM prediction) is quite strong for the new signatures. This may be used as an argument that prompt multifragmentation should not be treated simply as a short time limit for binary sequential decay.

This work was supported by the Polish State Committee for Scientific Research-French(IN_2P_3) agreement, (KBN Grant No. 2 P03B 139 14) and by the M. Skłodowska-Curie Fund (MEN/DOE-97-318). Calculations for this work were performed using the facilities of the CYFRONET Cracow Academic Computer Center.

REFERENCES

[1] H. Jaquaman *et al.*, *Phys. Rev.* **C27**, 2782 (1983).

[2] See *e.g.* J.D. Gunton, M. Droz, *Introduction to the Theory of Metastable and Unstable States, Lecture Notes in Physics* **183**, Springer-Verlag, Berlin-Heidelberg-New York-Tokyo.

[3] B. Borderie, *Ann. Phys.* (France) **17**, 349 (1992).

[4] J.A. Lopez, J. Randrup, *Nucl. Phys.* **A491**, 477 (1989).

[5] R. Trockel *et al.*, *Phys. Rev. Lett.* **59**, 2844 (1987).

[6] A.J. Cole *et al.*, *Phys. Rev.* **C47**, 1251 (1993); D. Heuer *et al.*, *Nucl. Phys.* **A583**, 537 (1995).

[7] K. Grotowski, *Acta Phys. Pol.* **B24**, 285 (1993).

[8] W. Gawlikowicz, K. Grotowski, *Acta Phys. Pol.* **B22**, 885 (1991); *Nucl. Phys.* **A551**, 73 (1993).

[9] D. Drain *et al.*, *Nucl. Instrum. Methods* **A281**, 528 (1989).

[10] T. Barczyk *et al.*, *Nucl. Instrum. Methods* **A364**, 311 (1995).

[11] P. Pawłowski *et al.*, *Phys. Rev.* **C54**, R10 (1996).

[12] P. Pawłowski *et al.*, *Z. Phys.* **A357**, 342 (1997).

[13] R. Płaneta *et al.*, preprint, Cracow IF UJ, ZFGM-99-01.

[14] J. Péter *et al.*, *Nucl. Phys.* **A593**, 95 (1995).

[15] J. Cugnon *et al.*, *Phys. Lett.* **109B**, 167 (1982); M. Gyulassy *et al.*, *Phys. Lett.* **110B**, 185 (1982); G. Fai, J. Randrup, *Nucl. Phys.* **A404**, 551 (1983).

[16] Z. Sosin, preprint, Cracow IF UJ, ZFGM-99-03.

[17] B.G. Harvey, *Nucl. Phys.* **A444**, 498 (1985); A.J. Cole, *Z. Phys.* **A322**, 315 (1985); *Phys. Rev.* **C35**, 117 (1987); L. Tassan-Got, C. Stéphan, *Nucl. Phys.* **A524**, 121 (1991); D. Durand, *Nucl. Phys.* **A541**, 266 (1992); Z. Sosin *et al.*, *Acta Phys. Pol.* **B25**, 1601 (1994).

[18] J. Randrup, *Nucl. Phys.* **A307**, 490 (1979).

[19] R.J. Charity *et al.*, *Nucl. Phys.* **A483**, 371 (1988).

[20] W. Gawlikowicz, PhD Thesis, Cracow 1994.

[21] W. Gawlikowicz, *Acta Phys. Pol.* **B28**, 1687 (1997).

[22] See the SIR code, D. Heuer *et al.*, unpublished.

[23] Y.D. Kim *et al.*, *Phys. Rev. Lett.* **67**, 14 (1991).

[24] E. Bauge *et al.*, *Phys. Rev. Lett.* **70**, 3705 (1993).

[25] E. Cornel *et al.*, *Phys. Rev. Lett.* **75**, 1475 (1995).